Investigation of MHD instabilities in tokamak plasmas using biorthogonal decomposition of Mirnov coil data

Habib Mehrniya , Mohammad Kazem Salem *, Ahmad Salar Elahi

Plasma Physics Research Center, Science and Research Branch, Islamic Azad University, Tehran, Iran.

***Corresponding author**: mkssalem@gmail.com

Abstract:

Spatiotemporal signal analysis is essential in investigating magnetic fluctuations of tokamak plasmas. Signal analysis of Mirnov coils through biorthogonal decomposition (BD) can reveal the spatial structure and time evolution of magnetohydrodynamic (MHD) instabilities in a tokamak. This technique is comparable to singular value decomposition in terms of formulation. The present study calculates the probability of instability modes' presence and identifies the dominant modes using the method above. Moreover, the relationship between the singular value entropy as a signal characteristic and magnetic field oscillations of Mirnov coils in the IR-T1 tokamak is investigated. This study evaluated the presence of active modes with and without applying a resonant helical field. The results indicate that when $L = 2$ and $L = 3$ are applied independently, the probability of $m = 2$ and 3 active modes is greater than when the resonant helical field is absent. In contrast, by combining these two, the likelihood of the presence of these modes is reduced.

1. Introduction

Nuclear fusion is a significant energy source that is actively pursued by scientists. For stable operation, the plasma required for fusion in the tokamak machine must reach temperatures over 150 million Kelvin [1]. However, the increase in plasma density and current results in a series of instabilities that lead to plasma losses. When the increase in the tokamak plasma current exceeds the critical limit, perturbation instability develops in the tokamak plasma. As a result, the plasma expands, collides with the tokamak's wall, and eventually cools down. The underlying cause of such perturbations is nonlinear growth in tearing modes [2]. The perturbations cause plasma radius expansion and reduced plasma confinement time [3].

Magnetohydrodynamic (MHD) fluid modeling is commonly used to characterize the most severe instabilities, in which changes in the magnetic topological configuration at surfaces with a rational safety factor cause MHD instabilities in the tokamak plasma. Magnetic field lines break in rational surfaces, and their reconstructions produce magnetic islands with resistance instabilities such as tearing modes. The ultimate effects of tearing modes comprise both large and small perturbations. Small perturbations destabilize the plasma and diminish particle confinement, whereas large perturbations are highly dangerous and terminate plasma discharge [4, 5]. In tokamaks with circular cross-sections and high aspect ratios, these modes oscillate per equation $\exp(i(m\theta - n\phi))$, where m denotes the number of poloidal modes, and n represents the toroidal mode number [6].

An effective tool for detecting MHD modes is utilizing data from the magnetic fluctuations in Mirnov coils. Data processing techniques are often used to analyze the oscillations associated with the tokamak's tearing mode instabilities, such as Mirnov oscillations [7–11]. Modes must be detected using spatiotemporal signal processing to analyze MHD instabilities in plasmas. Consequently, it is vital to determine the spatial structure and temporal evolution of MHD instabilities in a tokamak machine so that the required measures can be implemented to ensure the stable performance of the tokamak plasma [9–13].

Various techniques are utilized for signal processing and mode detection. The present study uses biorthogonal decomposition (BD), essentially expanding definite functions in time and space. To this end, the present paper utilizes the BD technique for Mirnov coils in the IR-T1 tokamak machine to obtain mode structure indices and presence probability.

Table 1. IR-T1 tokamak parameters.

Parameters	Value
Toroidal field	< 0.9 T
Plasma current	< 40 KA
Discharge time	< 35 ms
Electron density	$0.7 - 1.5 \times 10^{13}$ cm^{-3}
Electron temperature	$150 - 230$ eV
Pressure before discharge	$2.5 - 2.9 \times 10^{-5}$ Torr

The BD method originated in nonlinear dynamics, where it was used to examine wave propagation in turbulent systems [14,15]. In terms of formulation, this method is comparable to SVD (singular value decomposition). The authors of [16] and [17] applied BD to FTU and IR-T1 tokamaks, extracted instability indices, and determined the instabilities' onset time. The technique was also employed by [18] and [19] to analyze the JET tokamak, and the SUPRE TORE Mirnov coil, respectively. Refs. [20] and [21] comprehensively analyzed Mirnov coils in the ASDX tokamak using BD to identify paired modes. The results of [21] are virtually identical to those presented in this article. Studies [22] and [23] utilized a combination of diagnostic detectors (Mirnov probes and soft X-ray [SXR]) and electron cyclotron emission (ECE) detectors to determine mode behavior.

The current study employs the BD technique to determine the dominant modes by analyzing the magnetic field fluctuations in Mirnov coils. The paper is structured as follows: The IR-T1 tokamak's structural characteristics are described in Section 2. BD and singular value decomposition (SVD) are discussed in Section 3. The results from experimental data of Mirnov coils in the IR-T1 tokamak are provided in Section 4. Section 5 summarizes the paper with a conclusion and provides additional remarks.

2. Experimental setup

A small tokamak, IR-T1, was constructed of stainless steel and lacked a first wall. The device was installed at the Plasma Physics Research Center of the Science and Research Branch of Islamic Azad University and operated under a hydrogen atmosphere. The tokamak had a circular cross-section and a high aspect ratio, comprised of an inner radius of 12.5 cm, a minor radius of $a = 12.5$ cm, and a major radius of $R = 45$ cm. Furthermore, it was outfitted with a poloidal array of 12 discrete Mirnov coils separated by the same distance from the poloid. The characteristics of IR-T1 are summarized in Table 1. Additionally, the tokamak possessed a resonant helical field (RHF) that influenced plasma confinement via an external magnetic field generated by two conductors wound around the chamber with a specified helicity. The minor radius for helical windings was estimated to be 21 cm ($l = 2$) and 22 cm ($l = 3$), whereas the major radius was 50 cm.

3. Methods

3.1 The biorthogonal decomposition

In the present study, the BD technique was applied to Chronos (temporal orthogonal modes) and Topos (orthogonal spatial modes) to examine the space-time evolution of a complex signal. Time-space symmetry provides access to the signal structure and deterministic dynamics and is considered a deterministic tool for a fully developed complex signal [17, 19]. From this perspective, it is important to note that the dynamics produced signals in certain spatial phases. Each spatial mode belongs to one coherent structure with temporal evolution. Assume a scalar quantity, such as $y(x,t)$ (e.g., the magnetic field component), whose temporal evolution can be measured simultaneously at M spatial locations. The signal is simulated at M spatial locations and N moments of time to generate the $(Y)_{ij}$ matrix as follows:

$$(Y)_{ij} = y(x_j, t_i); \quad i = 1, ..., N, \text{ and } j = 1, ..., M \quad (1)$$

$y(x_j, t_i)$ is expanded into a set of orthogonal modes through BD expansion as:

$$y(x_j, t_i) = \Sigma_{k=1}^{K} A_k \varphi_k(x_j) \psi_k(t_i) \quad (2)$$

and

$$\Sigma_{i=1}^{N} \psi_k(t_i) \psi_l(t_i) = \Sigma_{j=1}^{M} \varphi_k(x_j) \varphi_l(x_j) = \delta_{kl} \quad (3)$$

The decomposition can also be calculated via SVD as follows:

$$(Y)_{ij} = VSU^T \quad (4)$$

where V and U denote $N \times M(V^T V = I)$ and $M \times M(U^T U = I)$ matrixes, respectively, and I is a unitary matrix. In addition, the diagonal $M \times M$ matrix S comprises elements $S_{ij} = s_i \delta_{ij}$ with $s_i \geq 0$, which are singular values of $(Y)_{ij}$ placed in descending order. Furthermore, the singular values in S are square roots of the eigenvalues of $(Y)_{ij}(Y)_{ij}^T$ or $(Y)_{ij}^T(Y)_{ij}$ and are always real numbers. The eigenvectors of $(Y)_{ij}(Y)_{ij}^T$, which are the column vectors of V, are the signal's temporal evolution known as components (PCs) that are equal to the projection of $(Y)_{ij}$ along U.

The column vectors of the U matrix, also known as principal axes, resemble the signal's fixed image and can estimate the spatial composition of the signal. In addition, the spatial eigenmodes $\psi_k(t_i)$ and $\varphi_k(x_j)$ are termed Chronos and Topos, respectively. The A_k (weight)≥ 0 is the diagonal values S matrix in Eq. (2). The signal's spatiotemporal properties are extracted via BD from Eq. (2). This section will define energy and entropy among the three essential signal parameters (dimension, energy, and entropy). Global space and time functions must be employed to extract temporal and spatial information. Additionally, BD can be derived through singular value decomposition.

An important advantage of biorthogonal is its weight distribution analysis, which provides valuable information about linear combinations and spatiotemporal symmetries. As demonstrated below, SVD factorization estimates the energy of signals as the sum of the squared A_k:

$$E = \Sigma_{i=1}^{N} \Sigma_{j=1}^{M} (Y)_{ij}^2 = \Sigma_{k=1}^{K} A_k^2 \quad (5)$$
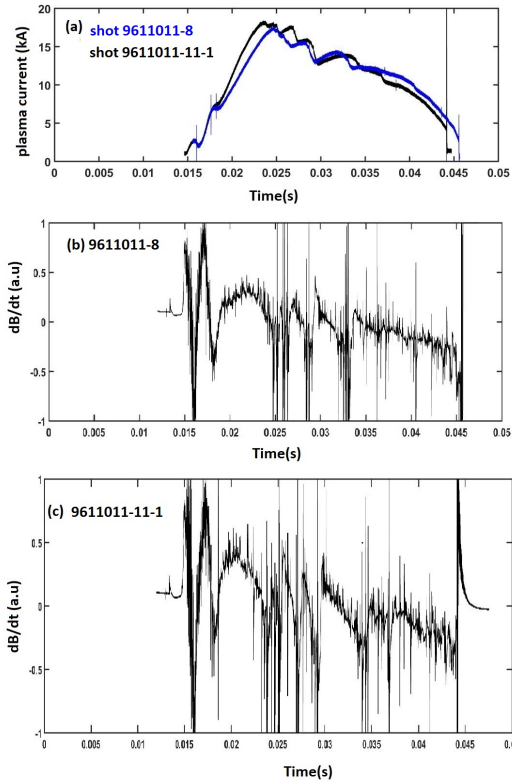
Figure 1. Plasma current and magnetic fluctuations (dB/dt) for IR-T1shot 9611011-8 and 9611011-11-1.

Figure 2. SVs(a) and PAs (b,c and d) of the Mironov coil signals obtained by BD Shot 9611011-8.
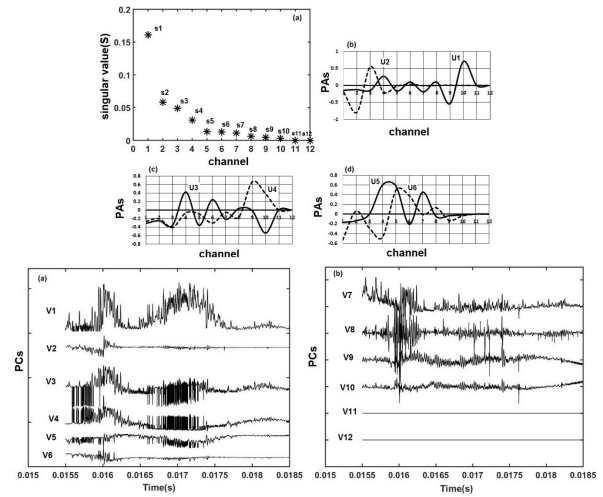
According to Eq. (5), a set of normalized squared singular values (dimensionless energy), $p_K = A_K^2/E$ is evaluated, which are the properties of a probability distribution $0 \leq p_k \leq 1$ and $\Sigma_{k=1}^{K} p_k = 1$, and is considered a useful tool for indicating the existence mode discussed in the following section.

Each Mirnov coil has a signal due to its single-mode perturbation expressed as $Y_k = A_k \cos(\theta_k - 2\pi \upsilon t)$, where θ_k (phase shift) is dependent on the topology (mode number) and position of the Mirnov coil, and υ is the temporal frequency of mode rotation. For M Mirnov coils in a poloidal cross-section and equally spaced positions, $\theta_k = 2\pi m/M(k-1)$ holds, where m is the poloidal mode number.

We consider Mirnov coils with known positions and a signal matrix with isochronous samples and Mirnov channels as rows and columns, respectively. We assume that all Mirnov coils are equally sensitive to magnetic perturbations. A theoretical mode (n,m), where n and m represent toroidal and poloidal mode numbers sampled by M coils at (ϕ, θ) (toroidal and poloidal angles), respectively, and a rotating frequency of sampled N times, yields the following expression:

$$(Yt)_{ij} = A \cos(m\theta_j \pm n\phi_j - \frac{2\pi\upsilon}{f_s}) \qquad (6)$$

Notably, due to the spatial symmetry and dimensions of the IR-T1 tokamak, we use $n = 1$ and ignore the toroidal effects. If the matrix Yt is factorized and trigonometric sum

formulas are applied, Eq. (6) can be rewritten as follows:

$$\begin{aligned}(Yt)_{ij} &= \cos(m\theta_j - \frac{2\pi\upsilon}{f_s}) \\ &= \cos(m\theta_j)\cos(\frac{2\pi\upsilon}{f_s}) + \sin(m\theta_j)\sin(\frac{2\pi\upsilon}{f_s})\end{aligned} \qquad (7)$$

$PA1t_{(n,m)}$ and $PA2t_{(n,m)}$ are the first two principal axes obtained by factorization of the $(Yt)_{ij}$ matrix. At this point, m is calculated by drawing the principal axes, counting their zero-crossings, and dividing by 2. Due to noise, plasma's principal axes and their theoretical counterparts are not identical. Considering the nature of principal axes and a single SVD principal axis, it is determined that the signal is generated over orthogonal basis vectors. Consequently, a mode likelihood is computed as follows:

$$Ln_{(n,m)} = \frac{|PA1t_{(n,m)} \cdot PA1e_{(n,m)}| + |PA2t_{(n,m)} \cdot PA2e_{(n.m)}|}{2} \qquad (8)$$

where $\cdot$ is the scalar multiplication between vectors of experimental and theoretical principal axes, and the experimental principal axes are projected on their theoretical ones. In addition, the mode likelihood is estimated as the absolute projection value of the first and second couple, resulting in a limited likelihood. According to Eq. (8), the likelihood value ranges from zero to one. The first case is orthogonally complete, and the second represents the identity case between the experimental and theoretical principal.

3.2 MHD instability indicators

Since the voltage across the coils is proportional to the derivative time of magnetic flux, the frequency determines the sensitivity of Mirnov coils to magnetic field perturbations. All Mirnov coils are assumed to have the same sensitivity to magnetic perturbations to improve theoretical principal axes. Thus, the theoretical principal axes are computed by assuming $A = 1$ in Eq. (6), and RMS normalization is performed. The results must be post-processed after signal normalization and SV decomposition to generate suitable MHD indicators.
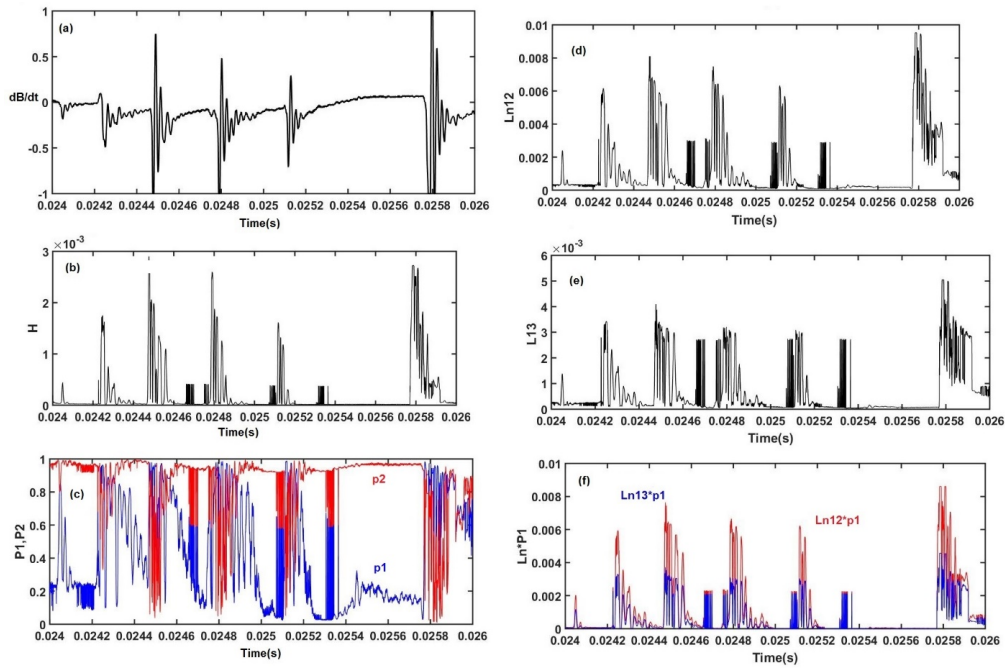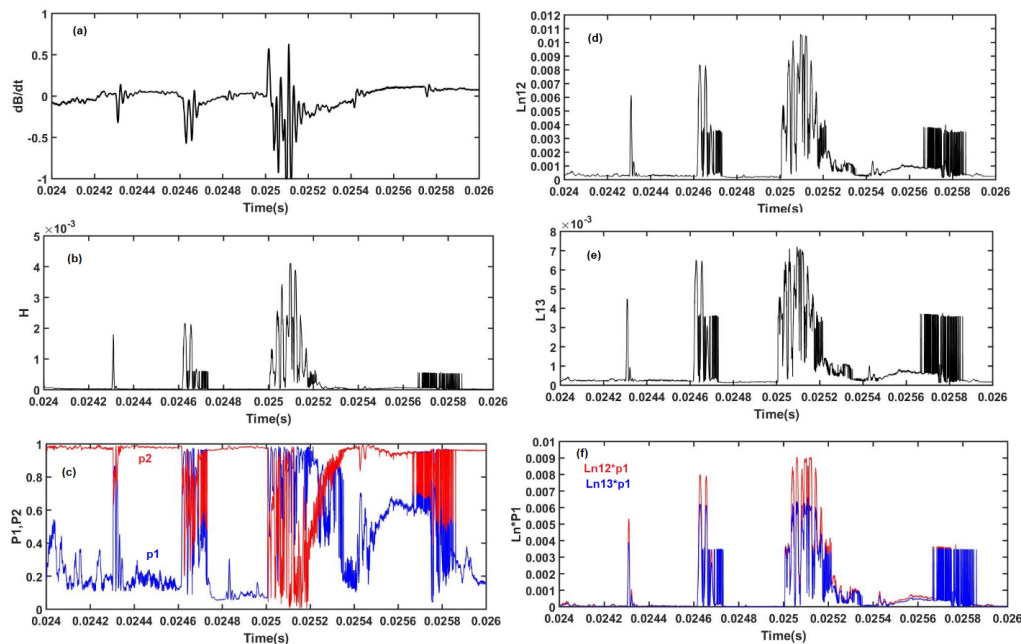
Figure 3. (a): Mirnov coil data, (b):H Entropy, (c): P_1 and P_2 indicators, (d): $Ln(n = 1, m = 2)$ Likelihood, (e): $Ln(n = 1, m = 3)$ Likelihood and (f): P_1 weighted likelihoods for IR-T1 shot no.9611011-5 without RHF in the time during 24-26 ms.

The first post-processing is presented in Eq. (8). The likelihood of each mode is calculated and categorized using mode topology. They can be separated into couples by SV factorization if they have more than one active mode, whereas singular values, which are valid in the case of equispaced Mirnov coils (such as the IR-T1 tokamak), are described in detail in Ref. [5]. SV factorization converts amplitude data to singular values. Since the degree of order/disorder is a crucial signal parameter, it is essential to specify the corresponding entropy, also known as singular values entropy. The complete space-time signal structure is described by the global signal quantity (the global entropy) as follows:

$$H = -\frac{\Sigma_{k=1}^M p_k \log(p_k)}{\log(M)} \tag{9}$$

Figure 4. (a): Mirnov coil data plot, (b): H Entropy, (c): P_1 and P_2 indicators, (d): $Ln(n = 1, m = 2)$ Likelihood, (e): $(n = 1, m = 3)$ Likelihood and (f): P_1 weighted likelihoods for IR-T1 shot no.9611011-11-1 with RHF ($L = 2, n = 1$) in the time during 24-26 ms.
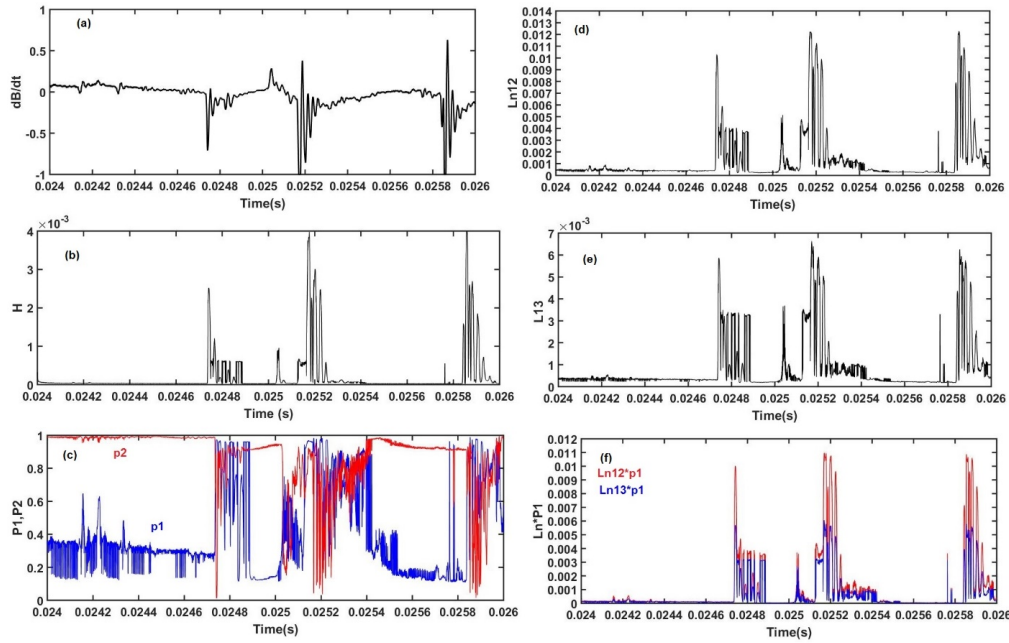
Figure 5. (a): Mirnov coil data plot, (b): H Entropy, (c): P_1 and P_2 indicators, (d): $Ln(n = 1, m = 2)$ Likelihood, (e): $Ln(n = 1, m = 3)$ Likelihood and (f): P_1 weighted likelihoods for IR-T1 shot no.9611011-8 with RHF ($L = 3$, $n = 1$) in the time during 24-26 ms.

Furthermore, the normalizing factor $(\log M)^{-1}$ is introduced to compare various signal entropies as the signal is obtained from different locations. A good indicator of instability is the entropy of singular values. With RMS signal normalization, the quantity of entropy is constrained between 0 and 1. H only becomes zero if a single eigenvalue is nonzero (when all signals are concentrated in the first structure). Alternatively, H becomes 1 if all eigenvalues are equal (when energy is equidistributed in all structures). Singular entropy is suitable for having a Boolean instability indicator [17]. Other markers are the relative squared magnitude of the first two pairs of principal axes:

$$P_1 = \frac{SV_1^2 + SV_2^2}{\Sigma_{i=1}^M SV_i^2} \tag{10}$$

$$P_2 = \frac{SV_3^2 + SV_4^2}{\Sigma_{i=3}^M SV_i^2} \tag{11}$$

Both quantities are limited between 0 and 1. If the value of Eq. (10) is closer to 1, the first mode of the signal is dominant; if the value of Eq. (11) is closer to 1, the second mode of the signal is dominant; and if either value is closer to 1, plasma performance is reduced.

4. Experimental results

In this section, an investigation is conducted using the BD method to analyze the magnetic fluctuation data from the Mirnov coils. To this end, pure hydrogen is injected into the tokamak at a pressure of 2.5 torrs. Plasma current and poloidal magnetic field fluctuations profile for tokamak plasma for two shots 9611011-8 and 9611011-11-1 are depicted in Fig. 1(a) . This figure shows that the separate applications of RHF ($L = 2$) and RHF ($L = 3$) have the same effect on the plasma flow, but their effect on magnetic fluctuations, eigenvalues of entropy, and probability of presence Fashions are different. Fig. 2(a) shows the eigenvalues corresponding to the principal axes (PAs) resulting from the BD method's analysis of Mirnov coils data for a typical shot of 9611011-8 in a time range of 24-26 ms.

The results show that the first pair of singular values have a significantly higher value than the other pairs, indicating that singular values have low entropy. The significant variation between the first pair of singular values and the remaining ones suggests that the first pair of principal axes (PAs) energy is significant, indicating the presence of an active magnetohydrodynamics (MHD) mode. Fig. 2(b, c, d) illustrates this shot's first three pairs of PAs in the 24-26 ms time range. The poloidal mode numbers for m = 2, 3, and 4 are found by counting the graphs with 0 at their intersection and dividing by 2. This method is ineffective for determining the poloidal mode number of the IR-T1 tokamak due to the multimode MHD activities.

The BD analysis method is recommended due to the simultaneous operation of multiple MHD modes (degenerate modes) in the magnetohydrodynamics activities of the IR-T1 tokamak plasma. The MHD instabilities are studied using a helpful index called the entropy of singular values, and an effective relationship between the amplitude of the poloidal magnetic field fluctuations and the entropy value is described. For instance, entropy rises with increasing magnetic field fluctuations between 24.4 and 24.6 ms (as shown in Fig. 3(a, b)) and falls to zero between 25.2 and 25.7 ms (when no magnetic field fluctuations occur). Fig. 3(c) illustrates two instability indicators P_1 and P_2, i.e., the relative energy value for the first two PA pairs between 24 and 26 ms.

The energy value of the first PA pair P_1 is greater than that of
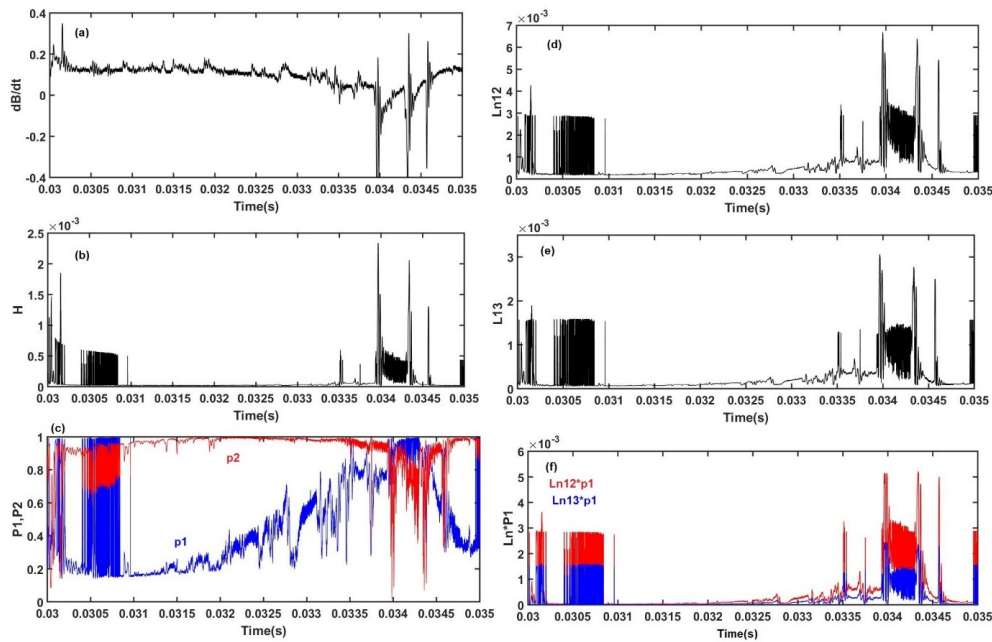
Figure 6. (a) Mirnov coil data plot, (b): H Entropy H, (c) p_1, p_2 indicators, (d) $Ln(n = 1, m = 2)$ Likelihood, (e) $Ln(n = 1, m = 3)$ Likelihood , and (f) p_1 weighted mode likelihoods for IRT-1 shot no 9611011-11-2 with RHF ($L = 2$ and $L = 3$ $n1$) in the time during 30-35 ms.

the second *PA* pair P_2 when instabilities occur in a range of times, such as between 24.4 and 24.6 ms. Multiple positive and negative peaks are depicted on the graphs for P_1 and P_2 to represent the two active modes operating concurrently. In addition, the dominant modes can be identified using $Ln_{(n,m)}$. Fig. 3(e, d) depicts the probability of the presence of two active modes ($n = 1$, $m = 2$) and ($n = 1$, $m = 3$) that are active with energy close to one another. Fig. 3(f) shows the normalized probability-weighted quantity P_1 obtained by multiplying $Ln_{(n,m)}$ by P_1, as well as the simultaneous activity for two ($n = 1$, $m = 2$) and ($n = 1$, $m = 3$) modes. The probability-weighted value P_1 can be introduced as a weighted factor to search the mode presence probability, which can classify the modes according to their activity rate. The mode $n = 1/m = 2$ is the primary mode, and the mode $n = 1/m = 3$ is the secondary mode, as shown in Fig. 3(f). Moreover, Figs. 4 and 5 illustrate the magnetic field fluctuations dB/dt, entropy indicators $H, P1, P2, Ln_{(n,m)}3n1, Ln_{(n,m)}2n1$, and $Ln_{(n,m)}(t)^*P1(t)$ for the 9611011-11-1 and 9611011-8 shots, respectively. For 9611011-11-1 and 9611011-8, the resonance helical magnetic fields (RHF) are ($l = 2$, $n = 1$) and ($l = 3$, $n = 1$), respectively. In addition, the results reveal the magnetic field fluctuations, the entropy of singular values, and relative energy values for the initial two *PA* pairs. In addition, using RHF, the probability of the present modes is modified in accordance with the normal case.

Figs. 4 and 5 depict the data graphs for shots No. 9611011-11-1 and 961011-8, respectively. Comparing Fig. 4(a, b) and Fig. 5(a, b) with Fig. 3(a, b) in the time interval of 25 to 25.2 ms reveals that magnetic fluctuations and the entropy of singular values increase with the application of RHF magnetic fields.

The comparison of Figs. 4(f) and 5(f) to Fig. 3(f) in the time

interval from 25 to 25. 2 demonstrates that the weighted probability of the P_1 index increases with the application of RHF, as does the simultaneous presence of two active modes $m = 2$ $n = 1$ and $m = 3$ $n = 1$. However, the likelihood of the presence of mode $m = 2$ $n = 1$ is greater than the probability of the presence of mode $m = 3$ $n = 1$, indicating that mode $m = 2$ $n = 1$ is the dominant mode. The results indicate that applying a resonant helical field improves the presence of active modes. This is evident when comparing Fig. 3(d, e), Fig. 4(d, e), and 5(d, e).

Shot No. 9611011-11-2 (Fig 6)continues Shot No. 9611011-11-1. In this shot, the combination of $l = 2$ and 3 fields was applied between a time interval of 30 and 35 ms. The constant P_2 index (Fig. 6(c)) indicates the absence of MHD modes, and the presence probability of the modes is almost zero in Fig. 6 (d, e) for the time interval 30 ms to 34 ms. In Fig. 6(c), the increase in P_1 (Eq. (10)) indicates the onset of plasma instability. The P_1 indicator remains relatively high between 34 and 34.5 ms, resulting in a more robust mode indicator. Notably, several negative and positive peaks in P_1 and P_2 confirm the continuous development and disappearance of the two modes. However, Fig. 6(d, e, f) indicate that the probability of mode presence is low when combined RHF ($l = 2$ and 3, $n = 1$) is applied.

5. Conclusion

The present study used the BD technique to examine data collected from an array of 12 Mirnov coils in the IR-T1 tokamak plasma. MHD instabilities were then investigated, and the corresponding mode number was assigned. The magnetic fluctuations corresponding to the rotating MHD modes were also examined by evaluating the SVD instability indices (H, P_1, and P_2).

The results revealed a strong correlation between the entropy of singular values (H), the relative square value for the first two *PA* pairs (P_1 and P_2), and plasma instabilities. In addition, the presence of two active ($m = 2$, $n = 1$) and ($m = 3$, $n = 1$) modes was determined, with the ($m = 2$, $n = 1$) mode being superior, by calculating the probability of the modes' presence in the tokamak. The activities of MHD modes were then evaluated with and without RHF. As a result, it was observed that the magnetic field fluctuations in the first case were lower than in the second, whereas the entropy of singular values increased. Using RHF ($l = 2$, $n = 1$) and RHF ($l = 3$, $n = 1$), the likelihoods $\ln_{(n,m)}$ of the ($n = 1$, $m = 2$) and ($n = 1$, $m = 3$) modes increased, while utilizing RHF ($l = 2$ and 3, $n = 1$) decreased the likelihoods of both modes.

Conflict of interest statement:
The authors declare that they have no conflict of interest.

References

[1] J. A. Wesson. "Hydromagnetic stability of tokamaks ". *Nuclear Fusion*, **18**:87, 1976.

[2] S. Elgriw and D. Liu. "Control of magnetic islands in the STOR-M tokamak using resonant helical fields". *Nuclear Fusion*, **51**:113008, 2011.

[3] A. Vannucci, I. C. Nascimento, and I. L. Caladas. "Disruptive instabilities in the discharges of the TBR-1 small Tokamak". *Plasma Physics and Controlled Fusion*, **31**:147, 1989.

[4] J. A. Wesson, R. D. Gill, M. Hugon, F. C. Schüller, J. A. Snipes, D. J. Ward, and D. V. Bartlett. "Disruptions in JET". *Nuclear Fusion*, **29**:641, 1989.

[5] R. Fitzpatrick and F. L. Waelbroeck. "Effect of electrostatic turbulence on magnetic islands". *Physics of Plasmas*, **15**:012502, 2008.

[6] J. A. Wesson. "Negative voltage spike in tokamak disruptions ". *Nuclear Fusion*, **30**:1011, 1990.

[7] P. V. Savrukhin, E. S. Lyadina, D. A. Martynov, D. A. Kislov, and V. I. Poznyak. "Coupling of internal m=1 and m=2 modes at density limit disruptions in the T-10 tokamak". *Nuclear Fusion*, **34**:317, 1994.

[8] H. Faridyousefi, M. K. Salem, and M. Ghoranneviss. "Study of MHD activities in IR-T1 Tokamak plasma using Hilbert-Huang transform". *Brazilian Journal of Physics*, **49**:864, 2019.

[9] H. Faridyousefi, M. K. Salem, and M. Ghoranneviss. "MHD mode identification from Mirnov coils signals in Tokamak via combination of singular value decomposition and Hilbert–Huang transform analysis methods". *Fusion Energy*, **39**:512, 2020.

[10] A. Salar Elahi and M. Ghoranneviss. "Effects of Resonant Helical Field on Plasma Internal Inductance in IR-T1 Tokamak". *Fusion Energy*, **28**:394, 2009.

[11] B. V. Waddell, B. Carreras, H. R. Hicks, J. A. Holmes, and D. K. Lee. "Mechanism for Major Disruptions in Tokamaks". *Physical Review Letters*, **41**:1386, 1978.

[12] CH. P. Ritz, E. J. Powers, T. L. Rhodes, R. D. Bengston, K. W. Gentle, H. Lin, P. E. Philips, A. J. Wootton, D. L. Brower, N. C. Luhman, W. A. Peebless, P. M. Schoch, and R. L. Hickok. "Advanced plasma fluctuation analysis techniques and their impact on fusion research (invited)". *Review of Scientific Instruments*, **59**:1739, 1988.

[13] K. V. Mardia, J. T. Kent, and J. M. Bibby. "Multivariate Analysis ". *Electronics*, :213, 1979.

[14] G. H. Golub and C. F. Van Loan. *Matrix Computations*. Hopkins Press, 1th edition, 1989.

[15] N. Aubry, R. Guyonnet, and R. Lima. "Spatiotemporal analysis of complex signals: theory and applications". *Journal of Statistical Physics*, **64**:63, 1991.

[16] C. Galperti. "Development of real-time MHD markers based on biorthogonal decomposition of signals from Mirnov coils". *Plasma Physics and Controlled Fusion*, **56**:114012, 2014.

[17] H. Mehrniya, M. K. Salem, and A. Salar Elahi. "Evaluation of Tokamak MHD instabilities by instability indices investigating such as entropy". *Fusion Energy*, **41**:19, 2022.

[18] C. Nardone. "Multichannel fluctuation data analysis by the singular value decomposition method. Application to MHD modes in JET". *Plasma Physics and Controlled Fusion*, **34**:1447, 1992.

[19] T. Dudok de Wit, A. L. Pecquet, J. C. Vallet, and R. Lima. "Enhancement of multichannel data in plasma physics by biorthogonal decomposition". *Physics of Plasmas*, **1**:3288, 1994.

[20] M. J. Hole and L. C. Appel. "A modulation model for mode splitting of magnetic perturbations in the mega ampere spherical Tokamak ". *Plasma Physics and Controlled Fusion*, **49**:1971, 2007.

[21] M. Schittenhelm. "Analysis of coupled MHD modes with Mirnov probes in Asdex Upgrade". *Nuclear Fusion*, **37**:1971, 1997.

[22] V. Igochine. "PHD Ttesis Technische Universitat Munshen ". , 2002.

[23] V. Igochine. "Simulation of NBI ion losses using GPUs ". *Nuclear Fusion*, **43**:1801, 2003.